JOURNAL OF THERMOPHYSICS AND HEAT TRANSFER
Vol. 10, No. 2, April–June 1996

Wideband Correlated-*k* Method Applied to Absorbing, Emitting, and Scattering Media

Ovidiu Marin* and Richard O. Buckius†
University of Illinois at Urbana–Champaign, Urbana, Illinois 61801

The correlated-*k* distribution method for widebands is developed and applied to participating media. The wideband *k*-distribution functions and the cumulative distribution functions provided by the Malkmus and the Goody narrow-band models, using the Edwards wideband model for line intensity and pressure broadening parameters, are compared. This work shows that the Malkmus and Goody models provide wideband absorptivities that are within 12% over the entire range of governing parameters. Limiting and approximate forms for the cumulative distribution function for the Malkmus formulation are presented. The correlated-*k* method is applied to problems involving absorbing, emitting, and scattering media, and the results using the gas models are compared. The wideband absorption for emission values obtained for the participating medium are within the same range of 12%. This work concludes that thermal transport applications can use the analytical forms provided by the Malkmus model combined with the parameters developed by Edwards for the wideband model.

Nomenclature

A = wideband absorption, cm^{-1}
a_1, a_2, a_3 = numerical parameters in error function approximation
B = pressure broadening parameter, $\pi b/d$
b = line half-width, cm^{-1}
d = line spacing, cm^{-1}
$f(k)$ = absorption coefficient distribution function or inverse transmission function
$g(k)$ = cumulative distribution function
$H_3(x)$ = Hermite polynomial
$h(k)$ = general spectral function
$I_0(x)$ = Bessel function
i = intensity, W/(m^2 sr)
i'^* = scattering-band absorption intensity
k = absorption coefficient, m^2/g
L = layer thickness, m
p = parameter in error function approximation
R = ratio, s_{max}/s_{min}
$S(x)$ = scattering source term
s = line intensity divided by line spacing, $\bar{s}/d$, m^2/g
$\bar{s}$ = line intensity, cm^{-1}/(g/m^2)
s_{max} = maximum line intensity, m^2/g
s_{min} = minimum line intensity, m^2/g
T = temperature, K
t_S = optical depth with respect to particle characteristics, $(k_S + \sigma_S)y$
u = mass path length, g/m^2
w = weight factor for Gaussian integration
x = variable
α = integrated band intensity, cm^{-1}/(g m^{-2})
$\alpha_1, \alpha_2, \alpha_3, \alpha_4$ = numerical parameters in the approximation of cumulative distribution function
$\alpha'_0, \alpha'_1, \alpha'_2, \alpha'_3, \alpha'_4$ = numerical parameters in the curve-fitted expression of the cumulative distribution function
$\beta_{i,j}$ = parameters in the curve-fitted expression of the cumulative distribution function
γ = parameter, $k_G/(k_S + \sigma_S)$
$\Delta\nu$ = wave number interval, cm^{-1}
ε = emissivity
ε' = directional emissivity
ε^* = wideband absorption for emission
θ = angle
κ = nondimensional absorption coefficient, k/s_{max}
μ = cos θ
ν = wave number, cm^{-1}
ν_0 = band center wave number, cm^{-1}
σ = scattering coefficient, m^2/g
χ = the band center optical depth, us_{max}
ω_d = bandwidth parameter, cm^{-1}
ω_S = particle scattering albedo, $\sigma_S/(k_S + \sigma_S)$

Subscripts

G = gas
Goody = Goody model
i, j = summation parameters
Malkmus = Malkmus model
max = maximum
min = minimum
nb = narrow band
S = scattering component
wb = wideband
ν = wave number dependent

Superscripts

$'$ = directional
* = wideband dependent
$\pm$ = positive and negative direction

Received June 15, 1995; revision received Sept. 5, 1995; accepted for publication Sept. 6, 1995.

*Research Assistant, Department of Mechanical and Industrial Engineering, 1206 West Green Street.
†Richard W. Kritzer Professor, Department of Mechanical and Industrial Engineering, 1206 West Green Street. Member AIAA.

Introduction

THE direct solution of the equation of transfer generally requires detailed information regarding the spectral de-

pendence of the absorption and scattering processes. With this spectral information the integration of equation of transfer over a wave number interval can be performed. Since the absorption coefficient of real gases is highly variable within the vibration–rotation bands, the quantification of radiative transport phenomena becomes very difficult. Various levels of approximation have been developed to quantify the gas properties within certain frequency intervals. The main difference between these methods is the magnitude of the frequency interval, varying from line-by-line methods to entire wideband approaches.

The line-by-line method, although it is an exact approach, requires a major computational effort, and this makes it unfeasible for most thermal transport applications. An alternate solution for nongray gaseous absorption problems is provided by narrow-band models. The concept of a narrow-band approach is to model the line strength variation over the wave number range of the band. Elsasser[1] provided a simple narrow-band model, which assumed all lines in a band are identical and equally distributed. Statistical models[2] proved to describe many gas bands more accurately. Plass[2] compares various models, extending the statistical model to include a random superposition of Elsasser bands. Ben-Aryeh[3] applied the statistical model to the 4.3-μm CO_2 band at high temperatures, showing good agreement with experimental measurements and theoretical predictions. The narrow-band models used most extensively were developed by Goody[4] and Malkmus.[5] The basic difference between the two models consists of the line intensity distribution function: Goody considered an exponential decay of the line intensity, whereas Malkmus used an exponential tailed s^{-1} distribution. The latter model accounts for more low intensity lines in the band, which is more accurate for certain bands.

Goldman and Kyle[6] compared the results given by narrow-band models with line-by-line calculations for specific ozone and water vapor bands. The results show good agreement for the two methods, but not a very good agreement with the measurements. This aspect might be attributed to the limitations of the experimental facilities at that time, but the results show the capabilities of band models to approximate the actual phenomena. Hartmann et al.[7] compare the results provided by line-by-line calculations with the Malkmus model applied to water vapor. The narrow-band parameters are generated from the line-by-line analysis. The results show that the absorptivities calculated using band models are about 10% greater than line-by-line calculations.

In addition to narrow-band models, wideband models have been developed, which give representations of entire bands. Edwards,[8] Edwards and Menard,[9] and Edwards and Balakrishnan[10] assumed an exponential line distribution and a constant pressure broadening parameter for the wideband. The method prescribes values for wideband parameters for each gas as well as the dependence of these parameters with temperature and pressure. These band models substantially reduce the computational effort of solving gas problems and combined gas-particle applications. Buckius[11] solved the radiative heat transfer problem for a nongray gas in the presence of scattering with the Edwards wideband model in the large pressure limit. An alternative approach to this problem uses the mean photon path length method,[12] which is an average length of photon travel within a scattering medium. The approach leads to significant computational savings and is most useful in Monte Carlo simulations.

An alternative approach to band models is given by the correlated-k (referred to as c-k hereafter) method.[13–16] The method replaces calculations on frequency domain with distribution functions for the absorption coefficient. The distribution function has been determined by various approaches. Arking and Grossman[17] present the absorption coefficient distribution function for numerous line and band models. West et al.[18] describe different practical methods of mapping the absorption coefficient given by line-by-line calculations into a distribution function. Domoto[19] applied the inverse Laplace transform to narrow-band transmission functions to obtain analytical expressions for the absorption coefficient distribution function. Using line-by-line results and a numerical inverse Laplace transform, Zhu[20] calculated c-k coefficients for random narrow-band models. Wang and Shi[21] developed a closed-form solution for the wideband distribution function with the Edwards wideband model applied to the Malkmus narrow-band model. Curve-fitting methods were used to calculate the band parameters of certain bands. Using the wideband absorptivity relation developed by Morizumi,[22] Lee et al.[23] developed a reordered distribution for the absorption coefficient.

The primary goal of this work is to present an efficient solution methodology using the c-k approach for wideband analysis including scattering. The gas properties are modeled using the Edwards wideband model applied to both the Malkmus and the Goody narrow-band models. A difficulty in the use of the c-k approach is that the narrow-band distribution function for the Goody model cannot be expressed in closed form. This fact makes Gaussian quadrature integration necessary. The work evaluates the differences encountered in the calculation of gas and gas-particle radiative transfer properties for the Malkmus and Goody models. Approximate, yet accurate, expressions for the cumulative distribution function are presented.

Correlated-k Method for Thermal Radiation Calculations

Correlated-k Distribution

The c-k method is based on the concept that in the solution of the radiative heat transfer equation, for a small wave number interval, the radiative properties of a gas are not strongly dependent on the location of the absorption coefficient within the wave number range. The integration for a band is replaced by an integration of the absorption coefficient distribution function $f(k)$. The equivalence of the formulations is expressed as

$$\frac{1}{\Delta\nu}\int_{\Delta\nu} h[k(\nu)]\,\mathrm{d}\nu = \int_0^\infty h(k)f(k)\,\mathrm{d}k \tag{1}$$

where $f(k)$ is the distribution function of k. The distribution function also satisfies the condition

$$\int_0^\infty f(k)\,\mathrm{d}k = 1 \tag{2}$$

Band Models

The distribution function concept has been applied to narrow-band models. For thermal radiation calculations, narrow-band models that assume a random distribution of the lines in the band have proven to be the most useful. The difference between various random models consists of the line intensity probability function. Malkmus[5] assumed an exponential tailed s^{-1} line intensity distribution and the corresponding distribution function has been obtained in closed form by Domoto.[19] The distribution function of the absorption coefficient is dependent upon s and B as

$$f_{\mathrm{nb}}(k, s, B) = \left(\frac{sB}{4\pi k^3}\right)^{1/2} \exp\left[\frac{B}{4}\left(2 - \frac{k}{s} - \frac{s}{k}\right)\right] \tag{3}$$

The other commonly used narrow-band model, developed by Goody,[4] assumes an exponential probability function for the line intensity distribution. So far, no closed form has been found for Goody's random band model. Using the inversion theorem of the Laplace transform applied to transmission,

Domoto[19] found an expression for the distribution function in an integral form. In terms of the same dependence B and s, the distribution function is expressed as

$$f_{nb}(k, s, B) = \frac{\pi}{8}\left(\frac{s}{B}\right)^{1/2}\int_0^k \left\{\int_0^\infty I_0\left[(4Bx)^{1/2}\right] \times \exp\left[-\frac{sx^2}{4B(k-k')}\right] dx\right\} H_3\left[\left(\frac{sB}{4k'}\right)^{1/2}\right]\frac{1}{k'^2} \times \frac{1}{(k-k')^{1/2}}\exp\left(-\frac{kB}{s}\right)\exp\left(-\frac{sB}{4k'}\right)dk' \quad (4)$$

Although many bands have been quantified by the Goody model,[8] Goldman and Kyle[6] showed that the narrow-band model developed by Malkmus gives more accurate results than Goody's model for the 2.7-μm H_2O band when compared to line-by-line calculations.

Narrow-band models divide an entire rotation–vibration band into subintervals. A coarser level of spectral detail is described by wideband models, which assume a line intensity distribution and a pressure broadening parameter dependence over an entire band. Edwards[8–10] assumes the line intensity decays exponentially from ν_0 as

$$s = s_{max}\exp\left\{-\left[\frac{2(\nu-\nu_0)}{\omega_d}\right]\right\} \quad (5a)$$

for a symmetrical band and as

$$s = s_{max}\exp\left\{-\left[\frac{(\nu-\nu_0)}{\omega_d}\right]\right\} \quad (5b)$$

for bands where the band head is located at the upper or lower limit of the frequency interval. This model also assumes that the pressure broadening parameter is constant. The expressions in Eqs. (5) give an s^{-1} dependence for the probability function with the line intensity, which yields the wideband distribution function as

$$f_{wb}(k) = \frac{1}{\eta(R)}\int_{s_{max}/R}^{s_{max}}\frac{1}{s}f_{nb}(k)\,ds \quad (6)$$

where R is the ratio of the maximum and minimum line intensity in the band (s_{max}/s_{min}). From Eqs. (5), R can also be expressed as $R = \exp(\Delta\nu/\omega_d)$, where $\Delta\nu$ is the total wideband frequency interval.

Wang and Shi[21] developed the solution for the wideband distribution function using the Edwards wideband model in the Malkmus narrow-band model. This solution is

$$f_{wb}(\kappa)s_{max} = \frac{1}{\eta(R)}\frac{\exp(B)}{2\kappa}\left\{\operatorname{erf}\left[\frac{\sqrt{B}}{2}\left(\sqrt{\frac{1}{\kappa}}+\sqrt{\kappa}\right)\right] - \operatorname{erf}\left[\frac{\sqrt{B}}{2}\left(\sqrt{\frac{1}{R\kappa}}+\sqrt{R\kappa}\right)\right]\right\} + \frac{1}{\eta(R)}\frac{1}{2\kappa}\left\{\operatorname{erf}\left[\frac{\sqrt{B}}{2}\left(\sqrt{\frac{1}{\kappa}}-\sqrt{\kappa}\right)\right] - \operatorname{erf}\left[\frac{\sqrt{B}}{2}\left(\sqrt{\frac{1}{R\kappa}}-\sqrt{R\kappa}\right)\right]\right\} \quad (7)$$

where $f_{wb}(\kappa)s_{max}$ represents the nondimensional wideband distribution function in terms of the nondimensional absorption coefficient $\kappa = k/s_{max}$. As the minimum line intensity in the band $s_{min} = s_{max}/R$ approaches zero, corresponding to the limit $R \to \infty$, the distribution function approaches a delta function. For any finite R, the limit of $f_{wb}(\kappa)$ as κ goes to zero, is zero. If s_{min} is considered rigorously equal to zero, the distribution function becomes divergent in κ. This behavior requires a finite R for Eq. (7) to be integrable. No similar closed-form expression has been presented for Goody's model due to the specific form of the integrand.

Figure 1 presents the nondimensional wideband absorption coefficient distribution function for both Malkmus and Goody models. As a result of the exponential-tailed s^{-1} line intensity distribution function, the Malkmus model shown in Fig. 1 attributes a higher probability to small values of the absorption coefficient. Most curves in Fig. 1 use a value of $\eta(R) = 7$. This value corresponds to a ratio R of approximately 10^3, which is considered sufficiently large to characterize entire rotation–vibration bands.[21] As R increases from $\eta(R) = 2$ to $\eta(R) = 7$, the distribution function shifts to lower values of the absorption coefficient and, in order to preserve Eq. (2) to higher peak values, approaching the delta function as $R \to \infty$. From a physical perspective, this trend is justified by the presence of more low-intensity lines in the band.

Several practical values for the nondimensional B have been presented. For a constant R, the distribution function shifts to smaller values of κ as B decreases, increasing the proportion of small absorption coefficients in the band. Since small values for B provide less line overlap, there is a larger probability of small absorption coefficients. Large values of B, which reflect an increase in line overlap, tend to limit the nondimensional absorption coefficient in the range $(1/R, 1)$. Figure 1 indicates that the distribution function decreases more rapidly in the vicinity of $\kappa = 1$ for $B = 10$.

Cumulative Distribution Function

The distribution function is used to calculate the cumulative distribution function for a wideband. In terms of the nondimensional absorption coefficient, the cumulative distribution function is expressed as

$$g(\kappa) = \int_0^k f_{wb}(k')\,dk' = \int_0^\kappa f_{wb}(\kappa')s_{max}\,d\kappa' \quad (8)$$

and it represents the probability of occurrence for absorption coefficients smaller than κ.

Figure 2 presents the cumulative distribution function for the same cases as shown in Fig. 1, i.e., both the Malkmus and the Goody models. The differences between the two models are less distinctive than in Fig. 1 due to the additional integration. The same conclusions as for the distribution function comparison can be drawn. The Malkmus model has a higher

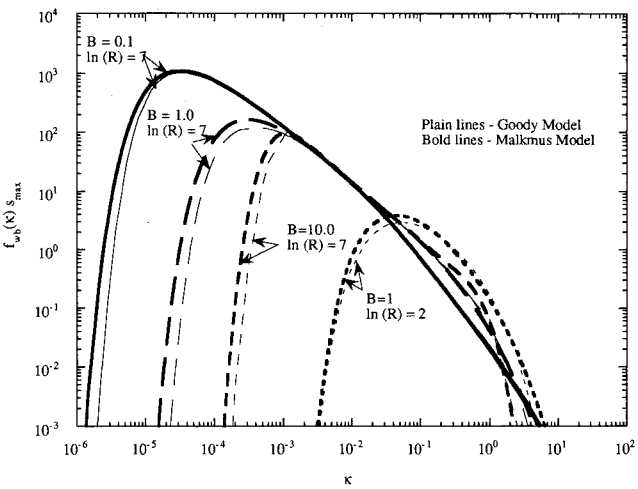

Fig. 1 Nondimensional distribution function using the Edwards wideband model with the Malkmus and Goody narrow-band models.

Table 1 Coefficients for the approximate cumulative distribution function in Eqs. (8c) and (8d)

	$\beta_{1,j}$		$\beta_{2,j}$		$\beta_{3,j}$		$\beta_{4,j}$	
j^a	$0.001 < B < 1.0$	$1.0 < B < 10.0$	$0.001 < B < 1.0$	$1.0 < B < 10.0$	$0.001 < B < 1.0$	$1.0 < B < 10.0$	$0.001 < B < 1.0$	$1.0 < B < 10.0$
0	21.4970	21.4971	6.4698	6.4690	19.9335	19.9336	−38.4266	−38.4270
1	50.4458	51.3543	17.2873	17.1955	29.7730	30.6215	−74.8679	−77.5492
2	−251.2901	−231.489	−68.7951	−69.2781	−218.5872	−200.2152	459.4210	400.1211
3	−235.7792	−75.5429	−31.7711	−24.6342	−197.4510	−49.5566	593.8412	120.4535
4	−408.5900	235.105	8.6279	66.3266	−377.3204	215.8386	1506.9760	−429.8971
5	−1246.601	147.789	−135.061	43.2328	−1152.481	123.9433	3960.2590	−217.9946
6	−1588.236	−57.6032	−263.4700	−9.8098	−1450.363	−56.1749	4902.0502	62.8147
7	−453.003	−74.6732	−130.6570	−28.1759	−400.7439	−70.4283	1615.2534	150.1507
8	1072.466	−36.8321	112.603	−13.1577	983.7614	−27.3857	−3186.021	79.0881
9	1542.366	3.2730	204.604	6.1804	1397.8735	4.9631	−5103.171	−19.8813
10	1042.760	20.3839	141.561	10.5758	938.5763	5.8304	−3775.539	−54.8543
11	431.5074	16.5137	57.2546	1.7031	386.2000	12.5505	−1713.144	−21.9417
12	114.9025	2.6544	14.5626	−6.5345	102.3168	2.9703	−501.3863	21.5502
13	19.3100	−9.1333	2.3001	−3.1483	17.1142	−6.2202	−92.6983	19.8170
14	1.8714	−9.5420	0.2066	7.2498	1.6513	−7.98757	−9.8785	−21.0811
15	0.0799	7.0739	0.0081	−2.6841	0.0702	5.2355	−0.4632	5.8005

[a]Summation index in Eq. (8d).

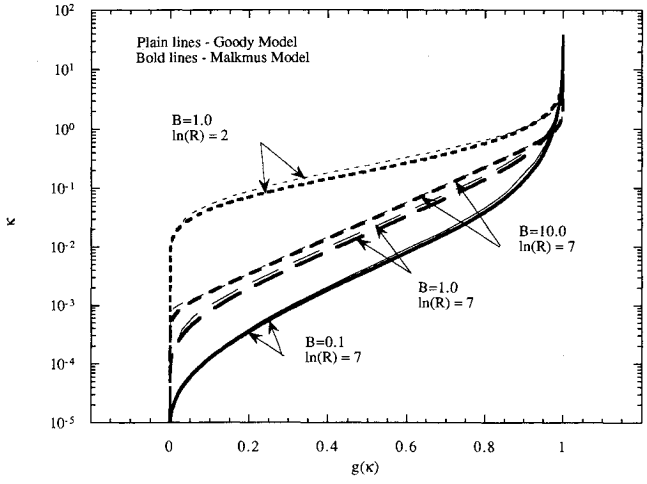

Fig. 2 Cumulative distribution function using the Edwards wideband model with the Malkmus and Goody narrow-band models.

probability of smaller values of the absorption coefficient. The cumulative distribution function spreads over a wider interval for the absorption coefficient as the pressure broadening parameter decreases. The ratio R has an important impact on the slope of the cumulative distribution function. As R decreases, the range of absorption coefficients in the band is reduced. Additionally, the distribution shifts towards higher values for absorption coefficient. In the limit $R \rightarrow 1$, the wideband cumulative distribution function becomes identical to the Malkmus narrow-band cumulative distribution function, for which there exists an analytical expression.[20]

To prescribe limiting forms for the cumulative distribution function, some limits of Eq. (7) are noted. In the limit as $B \rightarrow \infty$, the function $\kappa f_{wb}(\kappa)s_{max}/\delta(R)$ approaches a step function with a value 1 between $\kappa = 1/R$ and $\kappa = 1$, and zero elsewhere. Therefore, the cumulative distribution function in the limit $B \rightarrow \infty$ is

$$g(\kappa) = \frac{1}{\delta(R)} \int_{1/R}^{\kappa} \frac{1}{\kappa'} \, d\kappa' = \frac{\delta(\kappa R)}{\delta(R)} \tag{8a}$$

where κ is bounded by the interval $(1/R, 1)$. The results in Fig. 2 show that for a value of $B = 10$ the distribution function approaches the function given by Eq. (8a), which in semilog coordinates is a straight line. It is noted that in this limit the cumulative distribution function is independent of B.

In the limit $B \rightarrow 0$, the analysis of Eq. (7) shows that the term $\exp(B) \rightarrow 1$ and, more importantly, the terms of form $\sqrt{\kappa}$ and $\sqrt{\kappa R}$ can be neglected in the error function arguments. The justification for this approximation is that the cumulative distribution function shifts towards lower values of the absorption coefficient as B decreases. Therefore, the function $f_{wb}(\kappa)s_{max}$ will be dependent on the terms $\text{erf}(\frac{1}{2}\sqrt{B/\kappa})$ and $\text{erf}(\frac{1}{2}\sqrt{B/R\kappa})$ only. The resulting expression is then integrated when using the rational approximation for $\text{erf}(x)$,[24] $\text{erf}(x) = 1 - (a_1 t + a_2 t^2 + a_3 t^3)e^{-x^2}$, where $t = 1/(1 + px)$ is an expression that is valid for the entire domain $0 \le x < \infty$, with $a_1 = 0.3480242$, $a_2 = -0.0958798$, $a_3 = 0.7478556$, and $p = 0.47047$, the maximum error is less than 0.000025. With these assumptions, the expression for the cumulative distribution function becomes

$$g(\kappa) = \frac{2}{\delta(R)} \left\{ -\frac{1}{2} E_1(x^2) + \alpha_1 \left[\frac{1}{\sqrt{\pi}} e^{-x^2} - x \, \text{erfc}(x) \right] + \alpha_2 \frac{e^{-x^2}}{1 + px} + \alpha_3 \frac{e^{-x^2}}{(1 + px)^2} + \alpha_4 \, \text{erfc}(x) \right\}_{x = 1/2\sqrt{B/R\kappa}}^{x = 1/2\sqrt{B/\kappa}} \tag{8b}$$

where $\alpha_1 = 0.60136$, $\alpha_2 = -0.16547$, $\alpha_3 = -0.10403$, and $\alpha_4 = 0.6234$.

No similar simplifications have been found for intermediate values of B. An approximate expression has been developed for a large range of B $(0.001 \le B \le 10.0)$, with an identical form as Eq. (8b). In order to describe the cumulative distribution function, the coefficients of each term have been replaced with curve-fitted values as

$$g(\kappa) = \frac{2}{\delta(R)} \left\{ -\frac{\alpha_0'}{2} E_1(x^2) + \alpha_1' \left[\frac{1}{\sqrt{\pi}} e^{-x^2} - x \, \text{erfc}(x) \right] + \alpha_2' \frac{e^{-x^2}}{1 + px} + \alpha_3' \frac{e^{-x^2}}{(1 + px)^2} + \alpha_4' \, \text{erfc}(x) \right\}_{x = 1/2\sqrt{B/R\kappa}}^{x = 1/2\sqrt{B/\kappa}} \tag{8c}$$

where $\alpha_0' = 1.0003$, and α_1'–α_4' are functions of B, of the form

$$\alpha_i' = e^{\log_{10}(B)} \sum_{j=0}^{15} \beta_{i,j} [\log_{10}(B)]^j, \qquad i = 1\text{–}4 \tag{8d}$$

The coefficients $\beta_{i,j}$ are presented in Table 1. To accurately describe the behavior of the coefficients for all values of B,

the coefficients $\alpha_i'(i = 1-4)$ have been fit for low values of B ($B < 1.0$) and for high values of B ($B > 1.0$). The significance of the coefficient $\alpha_0' = 1.0003$, which can be taken equal to unity for most situations except those involving small optical paths and small B, is discussed later. The average error between the exact and curve-fitted expressions of $g(\kappa)$, with B in the interval from 0.001 to 10.0, is 0.7%. For values of B outside this interval, the limiting expression in Eq. (8a) should be used for $B > 10$, and Eq. (8b) for $B < 0.001$. The relatively high-order polynomial approximation has been used to reduce the error between the curve-fitted and the exact cumulative distribution function, especially for small values of B, where the cumulative distribution function spreads on a large interval and an accurate representation of the parameters α_i' is required. The use of the approximate forms in Eqs. (8a–8d) significantly reduces the CPU time required to calculate the cumulative distribution function. In radiative transport problems involving nonhomogeneous gas, the repeated calculations of the cumulative distribution function can become an important burden in the overall process, and this is one case where the approximate solutions developed earlier may be especially useful.

Correlated-k Results for Participating Media

Radiative heat transfer in various engineering applications requires consideration of nongray absorption by gases as well as scattering by particles. The effects of nongray absorption and isotropic scattering in a planar medium are considered for a medium that is homogeneous and isothermal at T. The intensities in the medium are represented by $i_\nu^{\pm}(t_S, t_{SL}, \omega_S, \gamma, \mu)$.[11] The gas contributions are expressed through the spectrally dependent k_G in the quantity $\gamma = k_G/(k_S + \sigma_S)$, which represents the ratio of the gas absorption coefficient to the scattering component extinction coefficient.

The combined contribution of gas and particles is the base value for this band intensity, and the pure scattering effect is subtracted from this value. This integrated difference over the band, representing the interaction of gas absorption and scattering, is defined as the total intensity for a single band

$$i^{\pm *}(t_S, t_{SL}, \omega_S, \chi, \mu) = \frac{1}{i_{\nu,b}(T)} \int_0^\infty [i_\nu^{\pm}(t_S, t_{SL}, \omega_S, \gamma, \mu) - i_\nu^{\pm}(t_S, t_{SL}, \omega_S, \gamma = 0, \mu)] \, \mathrm{d}\left(\frac{\nu}{\omega_d}\right) \tag{9}$$

The directional wideband absorption for emission is then

$$\varepsilon'^*(t_{SL}, \omega_S, \chi) = \text{⫽}(R) \int_0^1 \left\{ \varepsilon' \left[(1 + \gamma) t_{SL}, \frac{\omega_S}{1 + \gamma}, \chi \right] - \varepsilon'(t_{SL}, \omega_S, \chi) \right\} \mathrm{d}g \tag{10}$$

where $\varepsilon'(t_{SL}, \omega_S, \chi)$ is the directional emissivity of a pure scattering medium with ω_S from a layer with t_{SL} and $\varepsilon'[(1 + \gamma)t_{SL}, \omega_\nu/(1 + \gamma), \chi]$ represents the emissivity of a mixture of scattering particle and gas. Note that $(1 + \gamma)t_{SL}$ is the optical depth including all components and $\omega_\nu/(1 + \gamma)$ is the albedo of the mixture. In Eq. (9) the Planck function has been assumed to be constant over the entire band. In Eq. (10) the ratio $\Delta\nu/\omega_d$ has been replaced with ⫽(R). In a similar manner the total wideband absorption for emission is expressed as

$$\varepsilon^*(t_{SL}, \omega_S, \chi) = \text{⫽}(R) \int_0^1 \left\{ \varepsilon \left[(1 + \gamma) t_{SL}, \frac{\omega_S}{1 + \gamma}, \chi \right] - \varepsilon(t_{SL}, \omega_S, \chi) \right\} \mathrm{d}g \tag{11}$$

The integration in Eqs. (10) and (11) is solved using Gaussian quadratures. The cumulative distribution function presented in the previous section is represented in terms of Nth-order quadrature with weights w_i. This provides

$$\varepsilon'^*(t_{SL}, \omega_S, \chi) = \text{⫽}(R) \sum_{i=1}^{N} \left\{ \varepsilon' \left[(1 + \gamma) t_{SL}, \frac{\omega_S}{1 + \gamma}, \chi \right] - \varepsilon'(t_{SL}, \omega_S, \chi) \right\} w_i \tag{12a}$$

$$\varepsilon^*(t_{SL}, \omega_S, \chi) = \text{⫽}(R) \sum_{i=1}^{N} \left\{ \varepsilon \left[(1 + \gamma) t_{SL}, \frac{\omega_S}{1 + \gamma}, \chi \right] - \varepsilon(t_{SL}, \omega_S, \chi) \right\} w_i \tag{12b}$$

The weights and locations are determined with the cumulative distribution function.

Wideband Absorptivity

For the case of a pure gas and a single line of sight, Eqs. (1) and (10) with $h(k) = 1 - e^{-k\chi}$ yield the wideband absorption as

$$\frac{A(\chi)}{\omega_d} = \text{⫽}(R) \int_0^\infty (1 - e^{-\kappa\chi}) f(\kappa) s_{\max} \, \mathrm{d}\kappa = \text{⫽}(R) \int_0^1 (1 - e^{-\kappa\chi}) \, \mathrm{d}g \cong \text{⫽}(R) \sum_{i=1}^{N} (1 - e^{-\kappa_i\chi}) w_i \tag{13}$$

where the summation approximates the integral. The wideband absorption is evaluated for both the Malkmus and the Goody model. The analytical solution in Eq. (7) is compared to the numerical integration of the Goody model in Eq. (4). To assess the usefulness of the Malkmus closed-form solution as an approximation to the integral form of the Goody model, the results are presented as the difference defined as

$$\text{mean difference} = \frac{|A_{\text{Malkmus}} - A_{\text{Goody}}|}{\frac{A_{\text{Malkmus}} + A_{\text{Goody}}}{2}} 100(\%) \tag{14}$$

Figure 3 shows the variation of the mean difference with respect to the optical path for different values of B. The

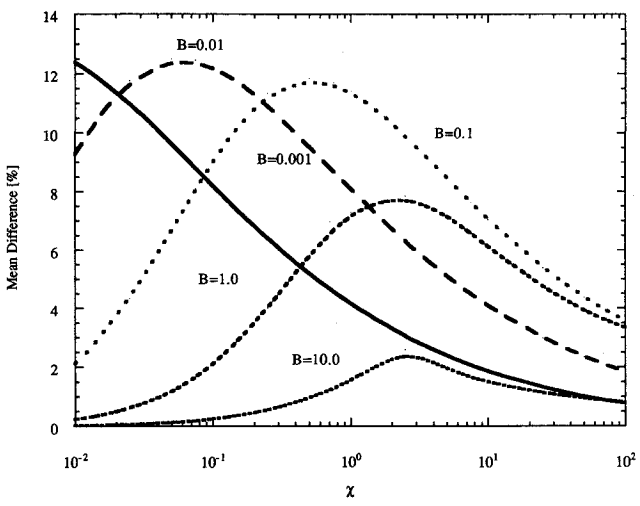

Fig. 3 Mean difference between the wideband absorptivity using the Edwards wideband model with the Malkmus and Goody narrow-band models.

differences between the two models are within 2% for large values of B ($B \geq 10$). As B decreases, the differences between the two models increase, but they are generally within 10% for a large range of B and χ. The Goody model systematically yields higher wideband absorptivity values than the Malkmus model. These results are consistent with the conclusions provided by the distribution function $f_{wb}(\kappa)s_{max}$, which indicated that the Goody model results in a higher probability for larger values of the absorption coefficient. The two models are within 5% for both small and large values of the optical path lengths, which correspond to the linear and square root regions as defined by Edwards.[8] The largest differences occur for intermediate values of the optical path length, which is a transition region between the linear and the square root regions. But even for these relatively narrow regions, the differences between the models were found to be within 12%. These differences between the models are relatively small compared to the approximations the band models inherently introduce, compared with experimental results, as indicated by Goldman and Kyle.[6]

The comparison between the wideband absorptivity using Goody's model and the approximate expressions in Eqs. (8) is also of interest. For most of the cases studied, the mean error obtained with the approximate Malkmus results from Eq. (8c) is the same as presented in Fig. 3, due to the accuracy of Eqs. (8). The only significant differences occur for low values of χ and B, where the error can be larger. These errors occur in regions where the wideband absorption has small values. The difficulty of accurately correlating small optical path and low-pressure phenomena has also been encountered by other researchers.[14,22] The maximum error was found to be 25% for $\chi = 0.01$ and $B = 0.1$ due to the shape of the cumulative distribution function for small values of B. The asymptotic behavior in the vicinity of $g(\kappa) = 1$ leads to large errors in the evaluation of κ, even when the errors in cumulative distribution function are very small. For example, with a value of $B = 0.001$, the average error between the wideband absorptivity calculated using Eq. (8b) and the exact integration is 9.33% in the interval $0.001 \leq \chi \leq 100.0$, with a maximum error of 32.8% for $\chi = 0.01$, while the average error of the distribution function itself is only 0.05%. The absorptivity error decreases as the optical path increases, becoming 0.4% for $\chi = 100.0$. When using a correction of 1.0003 multiplied to the exponential integral term in the cumulative distribution function, the maximum error of the wideband absorptivity becomes 4%, with an average error of 1.9%. This is the reason for the introduction of the coefficient α_0' in Eq. (8c). For calculations involving larger optical paths or larger values of B, α_0' can be taken equal to unity. The average error between the wideband absorptivity when using Eq. (8c) and the exact Malkmus cumulative distribution function is 1.8% for B in the range from 0.001 to 10.0. The error is generally less than 1% for values of $\chi \geq 1.0$.

The results obtained for the wideband absorption coefficient were used to determine the number of Gaussian quadratures required in Eq. (13). It has been found that for large values of B ($B = 10$), the number of quadratures can be quite small. To obtain results within 1% of the exact solution, only $N = 8$ is required. As B decreases, the cumulative distribution function becomes less steep, requiring a large range in absorption coefficients. This behavior requires an increase in quadrature points in order to secure the same accuracy. For $B = 0.1$ and lower, $N = 48$ has been used to achieve 1% error. This analysis has been done for a wide range of optical depths. The number of quadratures is significantly lower if the range excludes the low optical depth domain. Again, this is a result of the asymptotic shape of the cumulative distribution $g(\kappa)$ for large values of κ. The relative importance of the large absorption coefficient values increases for small values of the optical depth, and this requires an increase in the number of quadratures.

As noted, the parameter R is directly related to the spectral width of the band. Since the band absorptivity values are dependent on the spectral interval covered, R is an important parameter in the band calculation. Previous results simulate $R \to \infty$ using $\mathcal{A}(R) = 7$ or $R = 1096$, yet as χ increases, larger values of R are required. From a physical standpoint, this observation suggests that, for a given path length, only lines stronger than a certain value $s_{min} = s_{max}/R$ are contributing to the band absorption. In the calculations presented earlier, the maximum value χ is 100.0.

Scattering Calculations

Several methods can be used to calculate the radiative transport in Eq. (12). The results presented in this article use a Monte Carlo technique[25] and the results were compared to the exact solutions.[26] All of the results presented here were accurate to three decimal places. To achieve this accuracy the number of bundles has been varied with a minimum of 10^6. The absorption suppression method,[25] which tracks each bundle through the medium until reflection or transmission, was used. The strength of the bundle, initially equal to unity, is decreased after each scattering by a factor equal to the albedo. The total optical depth until reflection or transmission is summed simultaneously. For each absorption coefficient, determined by the quadrature locations and the cumulative distribution function, the total transmission or reflection is calculated by multiplying the effects of gas and pure scattering.

Using this method, the Goody and Malkmus models have been successively used to calculate the wideband absorption for emission including scattering. Figure 4 shows the wideband absorption for emission for the case $B = 0.1$, using different albedos and optical paths. For both large and small values of the band center optical depth the two models are similar in trend and value. For intermediate values of the band center optical depth, the differences increase, and for the entire interval the Goody model results are larger than the Malkmus model. The results for the case with only gas are presented by the slab band absorptance[27] as a reference. The differences between the two models were in the same range as the differences resulted from the wideband absorption calculations. For large values of B the two models give results within 2%. For smaller values of B the differences between the models are within 12%.

Figure 5 shows the variation of the wideband absorption for emission with scattering for the different problem parameters. Figure 5a shows the influence of t_{SL}, holding the albedo and B constant. For low values of t_{SL} the particle influence

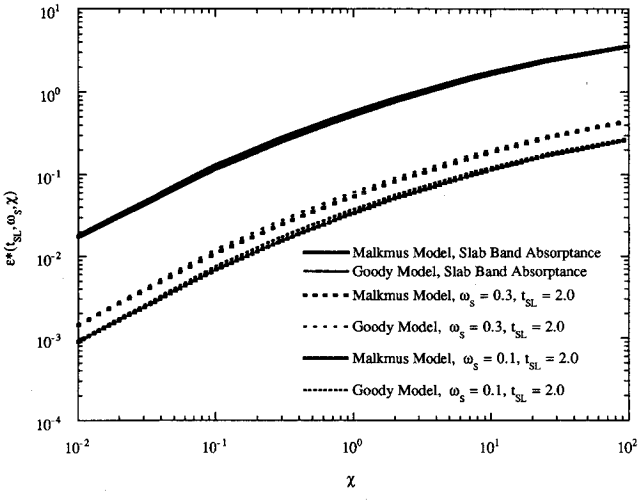

Fig. 4 Wideband absorption for emission using the Edwards wideband model with the Malkmus and Goody narrow-band models.

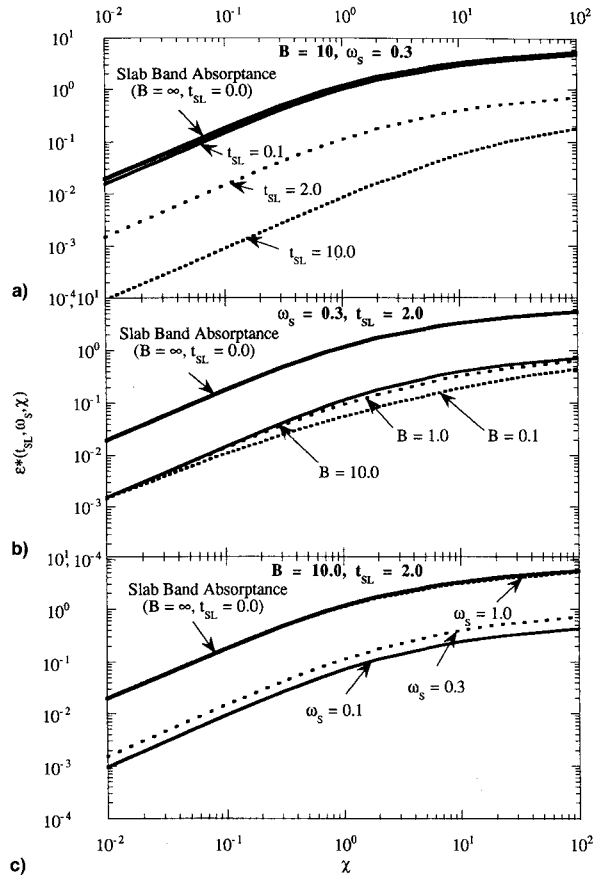

Fig. 5 Wideband absorption for emission using the Edwards wideband model with the Malkmus model. Influences of a) t_{SL}, b) B, and c) ω_S.

is negligible, with the values of the wideband absorption for emission approaching the slab band absorptance. For t_{SL} = 0.1, the average difference between the slab band absorptance and the wideband absorption for emission increases. As t_{SL} is further increased, the scattering phase becomes dominant. Between t_{SL} = 0.1, 2.0, and 10.0, the band absorption for emission drops by an order of magnitude for each. At the same time, for large values of t_{SL}, the linear absorption region covers a larger spectral interval.

Figure 5b shows the dependence of the band absorption for emission with respect to B. The emission values increase with increasing B. The largest difference occurs for a band center optical path $\chi \cong 1$, and the differences become smaller for both large and small values of χ. This dependence is explained by the curves in Fig. 2, where as B increases, the cumulative distribution functions become closer. The slope of the curves showing the band absorption for emission varies with the pressure broadening coefficients. As B decreases, the curves become less steep.

Finally, Fig. 5c presents the variation of the wideband absorption for emission when varying the particle albedo. A value of unity for albedo shows only a slight overall effect on the band emission. As the albedo decreases, the scattering phase becomes dominant in the process and the wideband absorption for emission decreases accordingly. By comparison with Fig. 5a, the decrease is of the same order of magnitude for all values of χ.

The same cases presented in Fig. 5 have been studied using the approximate form of the cumulative distribution function given in Eq. (8c). The errors for the wideband absorption for emission were in the same range as were the differences when using the exact cumulative distribution function. The use of the approximate equations for the cumulative distribution function in Eq. (8c) led to a significant reduction in CPU time compared with the numerical integration of Eq. (7).

The analysis presented in this article has used the same gas parameters for both the Malkmus and Goody models. In practice, the researcher has to determine these parameters according to the actual physical characteristics of the gas. For thermal radiative calculations Edwards[8] has studied gas absorption phenomena and employed the Goody narrow-band formulation. This work considered both the Malkmus model and Goody model and similar results were obtained as shown in Figs. 2–4. These relatively small differences suggest that for many engineering applications the same parameters developed by Edwards can be used in either of the two models. Although better accuracy could be obtained by developing a new set of model parameters,[21] it is recommended that Edwards[8] parameters be used with the Malkmus cumulative distribution functions presented in Eqs. (8) and Table 1. The expected deviation from exact numerical calculation is within 12%, with computational savings of at least a few orders of magnitude.

Conclusions

The wideband c-k method is applied to absorbing, emitting, and scattering media. The gas properties have been modeled using the Goody and the Malkmus narrow-band models with the Edwards wideband model.[8] To compare the results provided by the models, the absorption coefficient distribution functions as well as the cumulative distribution functions were presented. The Malkmus model gives a higher probability for small absorption coefficients, which better approximates the behavior of certain bands. Limiting as well as approximate analytical expressions for the Malkmus model cumulative distribution function have been developed indicating that, for large values of B, the cumulative function can be expressed in a simple logarithmic expression.

For a large parameter range, the Malkmus and Goody models yield results within 12% for the wideband absorptivity. The combined problem of gas absorption and isotropic particle scattering for a planar geometry was studied for both models. Again, the results were within the same difference. These results indicate that both models can be used in many practical applications without major differences. Furthermore, since only the theoretical parameters developed for a wideband model are available for a modified Goody model, it can be concluded that these parameters can be applied to the Malkmus model. The numerical integrations were performed using the Gaussian quadrature method, which provided an accuracy of 1%.

References

[1]Elsasser, W. M., *Heat Transfer by Infrared Radiation in the Atmosphere*, Harvard Meteorological Studies, No. 6, Harvard Univ. Press, Cambridge, MA, 1943.

[2]Plass, G. N., "Models for Spectral Band Absorption," *Journal of the Optical Society of America*, Vol. 48, No. 10, 1958, pp. 690–703.

[3]Ben-Aryeh, Y., "Spectral Emissivity Calculations by the Statistical Model Applied to the 4.3-μ Bands of CO_2 at High Temperatures," *Applied Optics*, Vol. 6, No. 6, 1967, pp. 1049–1055.

[4]Goody, R. M., "A Statistical Model for Water-Vapor Absorption," *Quarterly Journal of the Royal Meteorological Society*, Vol. 78, No. 2, 1952, pp. 165–169.

[5]Malkmus, W., "Random Lorentz Band Model with Exponential-Tailed S $^{-1}$ Line-Intensity Distribution Function," *Journal of the Optical Society of America*, Vol. 57, No. 3, 1967, pp. 323–329.

[6]Goldman, A., and Kyle, T. G., "A Comparison Between Statistical Model and Line by Line Calculation with Application to the 9.6-μm Ozone and 2.7-μm Water Vapor Bands," *Applied Optics*, Vol. 7, No. 6, 1968, pp. 1167–1177.

[7]Hartmann, J. M., Levi Di Leon, R., and Taine, J., "Line-by-Line and Narrow-Band Statistical Model Calculations for H_2O," *Journal of Quantitative Spectroscopy and Radiative Transfer*, Vol. 32, No. 2, 1984, pp. 119–127.

[8]Edwards, D. K., "Radiation Heat Transfer Notes," Hemisphere, New York, 1981.

[9]Edwards, D. K., and Menard, W. A., "Comparison of Models for Correlation of Total Band Absorption," *Applied Optics*, Vol. 3, No. 5, 1964, pp. 621–626.

[10]Edwards, D. K., and Balakrishnan, A., "Thermal Radiation by Combustion Gases," *International Journal of Heat and Mass Transfer*, Vol. 16, No. 1, 1973, pp. 25–40.

[11]Buckius, R. O., "The Effect of Molecular Gas Absorption on Radiative Heat Transfer with Scattering," *Journal of Heat Transfer*, Vol. 104, No. 3, 1982, pp. 580–586.

[12]Buckius, R. O., "Radiation Heat Transfer Using Mean Photon Path Lengths," *International Journal of Heat and Mass Transfer*, Vol. 25, No. 7, 1982, pp. 917–923.

[13]Gerstell, M. F., "Obtaining the Cumulative k-Distribution of a Gas Mixture from Those of Its Components," *Journal of Quantitative Spectroscopy and Radiative Transfer*, Vol. 49, No. 1, 1993, pp. 15–38.

[14]Goody, R., West, R., Chen, L., and Crisp, D., "The Correlated-k Method for Radiation Calculations in Nonhomogeneous Atmospheres," *Journal of Quantitative Spectroscopy and Radiative Transfer*, Vol. 42, No. 6, 1989, pp. 539–550.

[15]Goody, R., and Yung, Y. L., "Atmospheric Radiation. Theoretical Basis," Oxford Univ. Press, Oxford, England, UK, 1989.

[16]Lacis, A. A., and Oinas, V., "Correlated k Distribution and Nongray Absorption," *Journal of Geophysical Research*, Vol. 96, No. D5, 1991, pp. 9027–9048.

[17]Arking, A., and Grossman, K., "The Influence of Line Shape and Band Structure on Temperatures in Planetary Atmospheres," *Journal of the Atmospheric Sciences*, Vol. 29, No. 5, 1972, pp. 937–949.

[18]West, R., Crisp, D., and Chen, L., "Mapping Transformations for Broadband Atmospheric Radiation Calculations," *Journal of Quantitative Spectroscopy and Radiative Transfer*, Vol. 43, No. 3, 1990, pp. 191–199.

[19]Domoto, G. A., "Frequency Integration for Radiative Transfer Problems Involving Homogeneous Non-Gray Gases: The Inverse Transmission Function," *Journal of Quantitative Spectroscopy and Radiative Transfer*, Vol. 14, No. 9, 1974, pp. 935–942.

[20]Zhu, X., "The Correlated-k Coefficients Calculated by Random Band Models," *Journal of Quantitative Spectroscopy and Radiative Transfer*, Vol. 47, No. 3, 1993, pp. 159–170.

[21]Wang, W.-C., and Shi, G.-Y., "Total Band Absorptance and k-Distribution Function for Atmospheric Gases," *Journal of Quantitative Spectroscopy and Radiative Transfer*, Vol. 39, No. 5, 1988, pp. 387–397.

[22]Morizumi, S. J., "Comparison of an Analytical Model with Approximate Models for Total Band Absorption and Their Derivatives," *Journal of Quantitative Spectroscopy and Radiative Transfer*, Vol. 22, No. 5, 1979, pp. 467–474.

[23]Lee, P. Y. C., Raithby, G. D., and Hollands, K. G. T., "The 'Reordering' Concept of the Absorption Coefficient for Modeling Nongray Gases," *Radiative Heat Transfer: Current Research*, Vol. 276, American Society of Mechanical Engineers, New York, 1994, pp. 21–30.

[24]Abramowitz, M., and Stegun, I. A., "Handbook of Mathematical Functions," Dover, New York, 1965, p. 299.

[25]Walters, D. V., and Buckius, R. O., "Monte Carlo Methods for Radiative Transfer in Scattering Media," *Annual Review of Heat Transfer*, Vol. 5, 1992, pp. 239–262.

[26]Crosbie, A. L., "Apparent Radiative Properties of an Isotropically Scattering Medium on a Diffuse Substrate," *Journal of Heat Transfer*, Vol. 101, No. 1, 1979, pp. 68–75.

[27]Edwards, D. K., and Balakrishnan, A., "Slab Band Absorptance for Molecular Gas Radiation," *Journal of Quantitative Spectroscopy and Radiative Transfer*, Vol. 12, No. 10, 1972, pp. 1379–1387.